Title

Release and capture of bioactive oxidized phospholipids and oxidized cholesteryl esters during percutaneous coronary and peripheral arterial interventions in humans.

Journal

Journal of the American College of Cardiology, 63(19)

Authors

Ravandi, Amir
Leibundgut, Gregor
Hung, Ming-Yow
et al.

Publication Date

2014-05-20

DOI

10.1016/j.jacc.2014.01.055

Peer reviewed

Published in final edited form as:

J Am Coll Cardiol. 2014 May 20; 63(19): 1961–1971. doi:10.1016/j.jacc.2014.01.055.

Release and Capture of Bioactive Oxidized Phospholipids and Oxidized Cholesteryl Esters During Percutaneous Coronary and Peripheral Arterial Interventions in Humans

Amir Ravandi[1,3], **Gregor Leibundgut**[2,3], **Ming-Yow Hung**[3,7], **Mitul Patel**[3], **Patrick M. Hutchins**[4], **Robert C. Murphy**[4], **Anand Prasad**[3,5], **Ehtisham Mahmud**[3], **Yury I. Miller**[3], **Edward Dennis**[6], **Joseph L. Witztum**[3], and **Sotirios Tsimikas**[3]

[1]St. Boniface Hospital Research Centre, University of Manitoba, Winnipeg, Manitoba, Canada [2]University of Basel, Basel Switzerland [3]Department of Medicine, University of California San Diego, La Jolla, CA [4]Department of Pharmacology, University of Colorado Denver, Aurora, CO [5]Department of Medicine, University of Texas Health Science Center at San Antonio, San Antonio, Texas [6]Pharmacology and Chemistry and Biochemistry University of California, La Jolla, CA [7]Department of Internal Medicine, School of Medicine, College of Medicine, Taipei Medical University and Division of Cardiology, Department of Internal Medicine, Shuang Ho Hospital, Taipei Medical University, New Taipei City, Taiwan

Abstract

Objective—To assess whether oxidized lipids are released downstream from obstructive plaques following percutaneous coronary and peripheral interventions using distal protection devices.

Background—Oxidation of lipoproteins generates multiple bioactive oxidized lipids that affect atherothrombosis and endothelial function. Direct evidence of their role during therapeutic procedures, which may result in no-reflow phenomenon, myocardial infarction and stroke, is lacking.

Methods—The presence of specific oxidized lipids was assessed in embolized material captured by distal protection filter devices during uncomplicated saphenous vein graft, carotid, renal, and superficial femoral artery interventions. The presence of oxidized phospholipids (OxPL) and oxidized cholesteryl esters (OxCE) was evaluated in 24 filters using liquid chromatography, tandem mass spectrometry, enzyme-linked immunosorbent assays (ELISA) and immunostaining.

Results—Phosphatidylcholine (PC)-containing OxPL (PC-OxPL), including PONPC [1-palmitoyl-2-(9-oxononanayl) PC], representing a major PC-OxPL molecule quantitated within plaque material, POVPC [1-palmitoyl-2-(5-oxovaleroyl)-sn-glycero-3-phosphocholine] and PGPC (1-palmitoyl-2-glutaroyl-sn -glycero-3-phosphocholine) were identified in the extracted lipid portion from all vascular beds. Several species of OxCE, such as keto, hydroperoxide, hydroxy, and epoxy cholesterol ester derivatives from cholesteryl linoleate and cholesteryl arachidonate

Correspondence: Sotirios Tsimikas, Vascular Medicine Program, University of California San Diego, 9500 Gilman Drive, La Jolla CA, 92093-0682, Tel: (858) 534-6109, stsimikas@ucsd.edu..

were also present. The presence of OxPL was confirmed using enzyme linked immunoassays and immunohistochemistry of captured material.

Conclusion—This study documents the direct release and capture of OxPL and OxCE during percutaneous interventions from multiple arterial beds in humans. Entrance of bioactive oxidized lipids into the microcirculation may mediate adverse clinical outcomes during therapeutic procedures.

Keywords

oxidized phospholipids; oxidized cholesterol esters; lipoproteins; angioplasty

INTRODUCTION

Cardiovascular disease(CVD) remains one of the largest contributors to morbidity and mortality in the western world(1) and is progressively increasing in developing nations. Percutaneous interventions are increasingly being used for the treatment of acute coronary syndromes(ACS) and symptomatic obstructive coronary artery disease(CAD). Peri-procedural complications such as acute thrombosis and distal embolization and slow- or no-reflow phenomenon continue to remain limitations of procedural success. For example, despite the use of optimal anti-platelet therapies and statins, a significant number of patients develop peri-procedural MI, which identifies patients at worse long-term prognosis(2). Similarly, the risk of stroke/transient ischemic attack following carotid stenting is 1-4%, despite the use of embolic protection devices. In renal artery interventions, worsening of blush grade or decrease in frame count, presumably due to distal embolization, has been associated with ultrasound detected lipid-rich plaques and suboptimal clinical response(3). Although the etiology of peri-procedural events is multifactorial, identification of bioactive embolized material that mediate adverse clinical events may allow development of targeted therapies to further minimize adverse clinical events.

A large component of unstable atherosclerotic plaques is the lipid core (4), which is primarily composed of cholesterol crystals, oxidized LDL(OxLDL) and apoptotic and necrotic macrophage-derived foam cells(5,6). A large body of evidence shows that oxidized phospholipids(OxPL) and specifically phosphocholine containing OxPL(PC-OxPL) play a major role in the adverse biological activities of OxLDL(7-9). PC-OxPL represent a heterogeneous group of bioactive molecules that have been shown to promote cell death, platelet aggregation (10), monocyte recruitment and vasoconstriction. Polyunsaturated fatty acids(PUFA) on cholesteryl esters(CE) undergo similar modifications as the PUFA on phospholipids under oxidative stress. Such oxidized cholesteryl esters(OxCE), in which the PUFA is oxidized but not the cholesterol moiety, are also abundant in OxLDL and in atherosclerotic plaques(11-13) and have been shown to be biologically active initiating pro-inflammatory macrophage activation and promoting foam cell formation(14,15).

Plaque components released during iatrogenic plaque rupture may not only result in mechanical obstruction due to the size of the particles being larger than the microvessels, but also in functional obstruction mediated by vasoconstriction, platelet aggregation. neutrophil activation and inflammation mediated by bioactive oxidized lipids mechanically released

from the site of storage or sequestration(16-18). However, oxidized lipids released during percutaneous procedures may be the most clinically relevant as they may lead to adverse clinical events. Specifically, these compounds are small enough to pass through filter devices and impact the distal vessels and microcirculation. In this study, we hypothesized that performance of percutaneous interventions results in iatrogenic plaque disruption and/or rupture leading to distal release of bioactive oxidized lipids.

METHODS – Supplementary Section

RESULTS

All patients underwent clinically indicated interventions. Of the 24 distal embolic protection devices analyzed, 17 FilterWire EZ^{TM} were used in SVGs, 2 FilterWire EZ^{TM} in renal arteries, 2 Spider RX^{TM} in SFA and 3 Rx Accunet^{TM} in carotid arteries. The distal embolic protection devices were deployed prior to balloon angioplasty or stent placement in all cases. The first 12 filters were collected without accompanying clinical information. **Table 1** represents brief clinical background of the remaining 12 patients.

Analysis of unoxidized phospholipids and PC-containing oxidized phospholipids (PC-OxPL)

In order to identify PC-OxPL molecules within recovered filter material, known PC-OxPL standards PGPC, PONPC, PAzPC, POVPC, KOdiAPC and KDdiAPC were first separated on normal phase HPLC with precursor ion (m/z 184) scanning mode. **Figure 1A** shows the total ion chromatogram of the separated PC-OxPL standards. KOdiAPC(peak 1), PONPC(Peak 2) POVPC(peak 3) KDdiAPC(peak 4) PAzPC(peak 5), and PGPC(peak 6) eluted in order of mass and polarity. **Figure 1B** shows the molecular ions (positive ions) derived from the elution of standards corresponding to the precursor$[M+H]^+$ that were collisionally activated to generate the phosphocholine ion at m/z 184 showing m/z corresponding to known standards. **Figure 1 C-H** shows the elution time for each PC-OxPL standard with KOdiAPC having the earliest elution time with retention time of 17.5 min and PGPC eluting last with a retention time of 23.6 min.

We next analyzed the lipid extracts from embolic filter material by precursor ion scanning (m/z 184) allowing for identification of PC-OxPL. PC eluted earliest, followed by sphingomyelin(SM) and lysoPC(LPC) (**Figure 2**). Extracts from filter material showed an abundance of PC-OxPL molecules compared to extracts of non- oxidized, native LDL(nLDL) (**Figure 2A**). As an example, compounds eluting between 17.5 - 19.2 min represent a large component of fragmented PC-OxPL compared to nLDL **(Figure 2B)**. There were also other ions present in the plaque material not seen in nLDL (e.g. m/z 678, 822, 832, 850). Given that they eluted with other PC-OxPL molecules they likely represent both fragmented and polyoxygenated unsaturated PC molecules. For example, ion 678 based on mass and the elution pattern could represent the 18:0 fatty acid in the sn-1 position with C9 aldehyde moiety in the sn-2 position.

The retention time observed for the synthetic PONPC determined by the expected [M+H]+ at m/z 650.5**(Figure 2C)** was at 18.8 min and this specific ion transition (m/z 650→184)

was present in low abundance in nLDL but the most abundant ion observed in the SVG filter material elution in this retention time region**(Figure 2B).** Within plaque lipid extracts this approach was used to identify six oxidized phospholipids based on correlation of retention times to the oxidized standards available and to the appearance of these specific ion transitions at the appropriate retention times during analysis of the SVG material.

To increase our sensitivity by utilizing MRM scanning, the relative mass of PC-OxPL in the filters from various vascular beds was quantified by comparing to the internal standard (DNPC) that was added during lipid extraction. **Figure 3** demonstrates the MRM analysis of plaque material with peaks corresponding in retention time to known synthetic standards. OxLDL lipid extracts were also analyzed in the same way. We next compared the levels of PC-OxPL within different vascular beds and OxLDL. As a percent of identified PC-OxPL, the most abundant PC-OxPL was PONPC, which represented close to 50% of identified PC-OxPL across different vascular beds. This was also the case when lipid extracts from different vascular beds were analyzed showing PONPC as the most abundant PC-OxPL molecule with KDdiAPC representing the smallest fraction(**Figure 4).**

Utilizing both positive and negative ionization modes (positive for PC, SM, LPC and negative for PE, CL, PG, PS and PI) the total phospholipid profile in SVG samples was determined(**Figure 5A**). The most abundant phospholipids were of the PC class (37.82 %) followed by sphingomeyelin (SM) (31.06%), phosphatidylethanolamine (PE), lysophosphatidylcholine (lysoPC), PC-OxPL and lysophosphatidylethanolamine (lysoPE) with other phospholipids in lesser amounts. When compared to copper-oxidized LDL (OxLDL)(**Figure 5B**) the material recovered from SVGs had increased PE levels (15.40% vs. 1.63%, p=0.003). This could represent cellular debris in the recovered material since PE represents a larger portion of total phospholipids in macrophages and smooth muscle cells(19). Material from SVGs also contained more lysoPC (4.84% vs. 0.35%, p=0.0001), lysoPE (3.95% vs. 0.08%, p=0.0001), but less PC-OxPL (4.61% vs. 7.65%, p<0.0001) compared to OxLDL. It is important to note that the OxLDL sample had been dialyzed during preparation, leading to loss of lysoPC, and possibly other PL species, which influences these comparisons(20).

Additional oxidized phospholipid molecular species were present in these SVG samples when detailed analysis of the LC-MS/MS data were carried out. However, based on the relative abundance of an internal standard of all observed precursor ions of m/z 184, the majority of the ion current was accounted for by the 6 PC-OxPL described above. Additional detailed experiments are necessary to fully structurally characterize these species.

Analysis of oxidized cholesteryl esters (OxCE)

The presence of OxCE was further analyzed in four additional specimens using a semi-quantitative HPLC-MS/MS method. Data were collected in MRM mode using transitions corresponding to CE(18:2), CE(20:4), CE(22:6) and their major oxidation products, e.g. oxo-, hydroxy-, hydroxy-epoxy- and hydroperoxy-CEs, as previously described (21). The chromatograms of major CE and OxCE species revealed readily detectable quantities of CE oxidation products in each of the four samples(**Figure 6A).** The lack of positional specificity, specifically the equal abundance of 9- vs. 13-hydroperoxy-linoleic CE (the two

major peaks of the "hydroxy" series), suggested that the observed oxidation products were formed chiefly through non-enzymatic mechanisms, a result consistent with previous analyses of OxCE extracted from advanced peripheral lesions(21). It should be noted however that this observation does not preclude a contributing enzymatic component. The extent of CE oxidation varied markedly between samples. Certain chromatograms suggested a preponderance of oxidized species(**Figure 6A** upper panel) while others showed much less CE oxidation(**Figure 6A** lower panel). Semi-quantitative analysis of these results indicated the overall content of OxCE, as a percentage of the total CE, ranged from 11 to 92% in the individual filters(**Figure 6B**). Further analysis of individual CE species, and their oxidation products, revealed the major acyl component was 18:2 (linoleic), followed by 20:4 (arachidonic) and 22:6 (docosahexaenoic) (**Figure 6C**). The relative abundance of OxCE species followed directly from this acyl distribution; oxidation products of CE(18:2) were the most abundant followed by oxidation products of the less abundance, highly unsaturated species CE(20:4) and CE(22:6).

ELISA and immunochemical staining evidence of the presence of OxPL

Complimentary immunochemical techniques were used to demonstrate the presence of OxPL in the recovered plaque material, as well as the major plasma carriers of PC-OxPL, namely Lp(a) and plasminogen. This was accomplished by sonication of the filter materials in PBS, which were then directly plated on microtiter well plates, and the different moieties measured by ELISA techniques using antibodies specific for OxPL, apoB-100, apo(a), and plasminogen respectively, and the data expressed as relative light units (RLU) per 100 milliseconds. The mean±SD value for OxPL was 11,342±13,220, 8,114±9,524 for apo(a), 6,058±10,591 for apoB-100 and 2,103±1,602 for plasminogen, which represent values ~5X above background. Since different secondary antibodies were used in each assay, a direct comparison of the relative amounts of each component cannot be made.

Immunochemical methods also directly confirmed the presence of OxPL by immunostaining with antibody E06, which binds to the PC headgroup of oxidized but not normal phospholipids (**Figure 7**). In addition, prominent staining was noted for malondialdehyde(MDA) epitopes, representing another well-defined oxidation specific epitope(OSE), in this case epitopes of unstable 3-carbon dialdehyde that binds to proteins in the lesion.

DISCUSSION

This study documents the release and capture of OxPL and OxCE from multiple vascular beds following percutaneous arterial interventions using distal protection devices in hemodynamically-significant lesions from symptomatic patients. These findings were demonstrated consistently with a variety of techniques, including LC-MS/MS, ELISA and immunohistochemistry. The release of OxPL is consistent with the presence of these pro-inflammatory mediators in symptomatic lesions(7), the commonalities of their pro-atherogenic role in multiple vascular beds and their potential role in mediating peri-procedural and spontaneous clinical events.

The current study demonstrated that the majority of phospholipids identified consisted of unoxidized PC, PE and sphingomeyelin, with PC-containing OxPL representing ~5% of total phospholipid content. Remarkably, the distribution of phospholipids present in distal protection devices was very similar to in vitro generated OxLDL, which was produced by isolating LDL from normolipidemic donors and exposing it to copper sulfate. This provides further support for evidence that OxLDL is generated in vivo, and importantly in clinically relevant lesions that drive the need for treatment(5,21). The most abundant PC-containing OxPL was PONPC, which represented almost 50% of the entire mass of fragmented PC-containing phospholipids, and is likely derived from phospholipids containing linoleic acid based on its nonanoyl component that is fragmented at the carbon double bond present at this position. Other well-characterized bioactive PC-containing OxPL were also present, including POVPC, PGPC and KOdiAPC(7,22). Prior studies have demonstrated that these OxPL are present in OxLDL and in human atherosclerotic lesions and are associated with a variety of pro-inflammatory and pro-atherogenic properties. For example, they mediate endothelial/monocyte dysfunction and bioactivity(23,24) and are important ligands for scavenger receptors on macrophages(22,25) and platelets(10), which in turn lead to foam cell formation, release of inflammatory cytokines, and platelet aggregation(5,26,27).

The current observations from material derived from distal protection devices are generally consistent with prior data derived from autopsy material or endarterectomy specimens, in demonstrating the presence of a variety of OxPL(26,28). The relative proportions of OxPL in different studies are somewhat different, but this may be attributed to the fact that at autopsy or during endarterectomy, the entire plaque is removed and subjected to lipid extraction, as opposed to embolic material which could represent material from the most friable part of the plaque that is released following barotrauma of the devices used to dilate the lesions. These observations are also consistent with a comprehensive immunohistological study from our group in coronary autopsy specimens and carotid endarterectomy specimens(5), where antibodies directed to OSE, apoB and Lp(a) were used to immunostain intimal xanthomas, pathological intimal thickening, early and late fibroatheromas, thin cap fibroatheromas and ruptured plaques. It was demonstrated that OxPL were present in early lesions but increased substantially in content as lesions progressed. In particular, OxPL were abundantly present in foamy macrophages, under the fibrous cap and in the necrotic core and were most prevalent in ruptured plaques. These data are also consistent with our prior findings that OxPL plasma levels rise acutely following acute coronary syndromes(29) and post PCI(16) and are strongly associated with angiographically-determined CAD(30) and with native coronary artery chronic total occlusions(6). Furthermore, elevated levels of OxPL, as measured by the OxPL/apoB assay, independently predict 15-year CVD event rates and additionally re-classify approximately 30% of patients into either higher or lower risk categories, confirming their clinical relevance(31).

The most abundant OxCE molecules present in distal protection devices were isomers of singly- and doubly-oxidized forms of cholesteryl linoleate, CE(18:2), e.g. hydroxy- and hydroperoxy-CE(18:2). Similar oxidation products of CE(20:4) and CE(22:6) were detectable but present in much lower quantities. Recently, Hutchins et al(12) showed the presence of a variety of OxCE within atherosclerotic plaques from femoral artery

endarterectomy specimens that represented ~20% of the total CE pool. They also showed that OxCEs are mainly present at the lipid core of the plaque with imaging mass spectrometry. Interestingly, most of the oxidized fatty acyl groups were derived from CE(18:2), but curiously, not from triglycerides in the plaques. Truncated, ω-oxidized-CEs, such as C9- and C5-aldehydes, as well as hydroxy- and hydroperoxy-CE species were identified in plaque material. Intriguingly, in our study, aldehydes represented a minor OxCE fraction, while epoxy and hydroperoxy moieties constituted a majority of OxCE. This was in contrast to OxPL, the majority of which were aldehydes. This deviation in OxCE and OxPL molecular species found in distal protection devices may suggest the different mechanisms of CE and PL oxidation, for example enzymatic vs. non-enzymatic, and/or different susceptibility of CE and PL hydroperoxides to form breakdown aldehyde products. The 18:2 and 20:4 CE are the preferential substrate for 15-lipoxygenase, the enzyme present in human atherosclerotic lesions and important in *in vivo* LDL oxidation, as shown in murine atherosclerosis models(32). It has also been demonstrated that once OxCE are formed, the oxidized acyl chains can be hydrolyzed from OxCE and then re-esterified into phospholipids to form OxPL(33). Further, it is also possible that enzymatic processes, mediated for example by 15-lipoxygenase, first initiate CE peroxidation and then non-enzymatic pathways then predominate as the lesions progress and mature leading to accumulation of aldehydic products. The fact that we observed no positional specificity among OxCEs suggested that non-enzymatic oxidation was dominant but it certainly does not rule out enzymatic initiation or amplification of CE oxidation.

Clinical implications

These findings provide a novel mechanism for the benefit of distal protection devices in potentially reducing peri-procedural events, by preventing embolized plaque material with its cargo of OxPL and OxCE from entering the microcirculation. OxPL have acute detrimental effects on endothelial function(7,34), including increasing permeability by breaking down cell junctions and stress fibers, releasing pro-inflammatory cytokines such as IL-8 and MCP-1, quenching of nitric oxide and enhancing platelet aggregation. These effects may lead to attraction of pro-inflammatory cells, vasoconstriction and microvascular obstruction.

The use of distal protection devices, compared to human autopsy or endarterectomy specimens, allows plaque material to be obtained from the iatrogenic plaque rupture of specific lesions of defined geometry and it potentially represents the most clinically-relevant embolized debris. Furthermore, the filter pores are generally ~90-110μm in diameter and smaller-sized fragments and soluble mediators not attached to larger fragments will pass through the filter, as shown for oxidized lipids in venous samples collected post-PCI without distal protection(5,16,29).

Clinical evidence of the potential role of CE is provided by near infrared spectroscopy(35,36), which detects lipid rich plaque composed mostly of CE, and by intravascular ultrasound virtual histology that detects the lipid-rich necrotic core(37). It is not known if OxCE are imaged with near infrared spectroscopy. This study suggests that developing techniques to image OxCE within this larger pool of cholesteryl esters may

provide more precise risk stratification of peri-procedural events and spontaneous plaque rupture. It would also allow performance of studies to follow the natural history of the role of oxidized lipids in clinical event prediction, similar to the PROSPECT study(38), and to determine the efficacy of pharmacological agents. We have developed techniques to image these oxidized lipids in animal models using targeted nanoparticles containing oxidation-specific antibodies with nuclear and magnetic resonance imaging techniques(39) or using fluorescent protein-tagged oxidation-specific antibodies(40), that may ultimately be modified and coupled to invasive modalities as molecular imaging probes in humans. In animal studies of atherosclerosis regression, oxidized lipids are one of the first plaque components to disappear from the vessel wall and are subsequently replaced by collagen and smooth muscle cells as markers of plaque stabilization (40-42). Therefore, imaging changes in the oxidized lipid content of plaques may provide a unique and informative index of rapid changes in plaque composition, prior to anatomical plaque regression, that may reflect clinical benefit.

Future studies linking release of such OxPL with peri-procedural clinical events are needed to confirm this hypothesis. If this is indeed confirmed, therapeutic agents to target oxidized lipids, such as human and “natural” oxidation-specific antibodies(9,43), could be infused during ACS/STEMI or just prior to percutaneous interventions, to bind the released oxidized lipids and prevent their interaction with platelets and endothelial cells, thus potentially abrogating vasoconstriction, no-reflow phenomenon and thrombosis(16,29,30).

Limitations

Complete oxidized lipidomics of non-PC based OxPL was not performed and it is possible that non-PC based OxPL also have pathophysiological roles. However, PC-based PL are in the greatest abundance and the most well characterized. It is possible small changes in the oxidized lipid proportions may have occurred due to ex vivo oxidation despite the use of EDTA/BHT and careful handling, as suggested by Liu et al(44).

References

1. Roger VL, Go AS, Lloyd-Jones DM, et al. Heart disease and stroke statistics—2012 Update. Circulation. 2012; 125:e2–e220. [PubMed: 22179539]
2. Wang TY, Peterson ED, Dai D, et al. Patterns of cardiac marker surveillance after elective percutaneous coronary intervention and implications for the use of periprocedural myocardial infarction as a quality metric: A report from the National Cardiovascular Data Registry (NCDR). J Am Coll Cardiol. 2008; 51:2068–2074. [PubMed: 18498965]
3. Prasad A, Ilapakurti M, Hu P, et al. Renal artery plaque composition is associated with changes in renal frame count following renal artery stenting. J Invasive Cardiol. 2011; 23:227–31. [PubMed: 21646647]
4. Virmani R, Kolodgie FD, Burke AP, Farb A, Schwartz SM. Lessons from sudden coronary death: a comprehensive morphological classification scheme for atherosclerotic lesions. Arterioscler Thromb Vasc Biol. 2000; 20:1262–75. [PubMed: 10807742]
5. van Dijk RA, Kolodgie F, Ravandi A, et al. Differential expression of oxidation-specific epitopes and apolipoprotein(a) in progressing and ruptured human coronary and carotid atherosclerotic lesions. J Lipid Res. 2012; 53:2773–90. [PubMed: 22969153]
6. Fefer P, Tsimikas S, Segev A, et al. The role of oxidized phospholipids, lipoprotein (a) and biomarkers of oxidized lipoproteins in chronically occluded coronary arteries in sudden cardiac

death and following successful percutaneous revascularization. Cardiovasc Revasc Med. 2012; 13:11–9. [PubMed: 22079685]

7. Lee S, Birukov KG, Romanoski CE, Springstead JR, Lusis AJ, Berliner JA. Role of phospholipid oxidation products in atherosclerosis. Circ Res. 2012; 111:778–799. [PubMed: 22935534]
8. Lichtman AH, Binder CJ, Tsimikas S, Witztum JL. Adaptive immunity in atherogenesis: new insights and therapeutic approaches. J Clin Invest. 2013; 123:27–36. [PubMed: 23281407]
9. Miller YI, Choi SH, Wiesner P, et al. Oxidation-specific epitopes are danger-associated molecular patterns recognized by pattern recognition receptors of innate immunity. Circ Res. 2011; 108:235–48. [PubMed: 21252151]
10. Podrez EA, Byzova TV, Febbraio M, et al. Platelet CD36 links hyperlipidemia, oxidant stress and a prothrombotic phenotype. Nature Medicine. 2007; 13:1086–1095.
11. Fang L, Harkewicz R, Hartvigsen K, et al. Oxidized cholesteryl esters and phospholipids in zebrafish larvae fed a high cholesterol diet: macrophage binding and activation. J Biol Chem. 2010; 285:32343–51. [PubMed: 20710028]
12. Hutchins PM, Moore EE, Murphy RC. Electrospray MS/MS reveals extensive and nonspecific oxidation of cholesterol esters in human peripheral vascular lesions. J Lipid Res. 2011; 52:2070–83. [PubMed: 21885431]
13. Harkewicz R, Hartvigsen K, Almazan F, Dennis EA, Witztum JL, Miller YI. Cholesteryl ester hydroperoxides are biologically active components of minimally oxidized low density lipoprotein. J Biol Chem. 2008; 283:10241–51. [PubMed: 18263582]
14. Choi SH, Harkewicz R, Lee JH, et al. Lipoprotein accumulation in macrophages via toll-like receptor-4-dependent fluid phase uptake. Circ Res. 2009; 104:1355–63. [PubMed: 19461045]
15. Kadl A, Sharma PR, Chen W, et al. Oxidized phospholipid-induced inflammation is mediated by Toll-like receptor 2. Free Rad Biol Med. 2011; 51:1903–1909. [PubMed: 21925592]
16. Tsimikas S, Lau HK, Han KR, et al. Percutaneous coronary intervention results in acute increases in oxidized phospholipids and lipoprotein(a): short-term and long-term immunologic responses to oxidized low-density lipoprotein. Circulation. 2004; 109:3164–70. [PubMed: 15184281]
17. Gregorini L, Marco J, Heusch G. Peri-interventional coronary vasomotion. J Mol Cell Bio. 2012; 52:883–9.
18. Leineweber K, Bose D, Vogelsang M, Haude M, Erbel R, Heusch G. Intense vasoconstriction in response to aspirate from stented saphenous vein aortocoronary bypass grafts. J Am Coll Cardiol. 2006; 47:981–6. [PubMed: 16516081]
19. Sahu S, Lynn WS. Lipid composition of human alveolar macrophages. Inflammation. 1977; 2:83–91. [PubMed: 617805]
20. Steinbrecher UP, Parthasarathy S, Leake DS, Witztum JL, Steinberg D. Modification of low density lipoprotein by endothelial cells involves lipid peroxidation and degradation of low density lipoprotein phospholipids. PNAS. 1984; 81:3883–7. [PubMed: 6587396]
21. Tsimikas S, Miller YI. Oxidative modification of lipoproteins: Mechanisms, role in inflammation and potential clinical applications in cardiovascular disease. Curr Pharma Des. 2011; 17:27–37.
22. Podrez EA, Poliakov E, Shen Z, et al. Identification of a novel family of oxidized phospholipids that serve as ligands for the macrophage scavenger receptor CD36. J Biol Chem. 2002; 277:38503–16. [PubMed: 12105195]
23. Watson AD, Leitinger N, Navab M, et al. Structural identification by mass spectrometry of oxidized phospholipids in minimally oxidized low density lipoprotein that induce monocyte/endothelial interactions and evidence for their presence in vivo. J Biol Chem. 1997; 272:13597–607. [PubMed: 9153208]
24. Subbanagounder G, Leitinger N, Schwenke DC, et al. Determinants of bioactivity of oxidized phospholipids : Specific oxidized fatty acyl groups at the sn-2 position. Arterioscler Thromb Vasc Biol. 2000; 20:2248–2254. [PubMed: 11031211]
25. Boullier A, Friedman P, Harkewicz R, et al. Phosphocholine as a pattern recognition ligand for CD36. J Lipid Res. 2005; 46:969–76. [PubMed: 15722561]
26. Ravandi A, Babaei S, Leung R, et al. Phospholipids and oxophospholipids in atherosclerotic plaques at different stages of plaque development. Lipids. 2004; 39:97–109. [PubMed: 15134136]

27. Podrez EA, Poliakov E, Shen Z, et al. A novel family of atherogenic oxidized phospholipids promotes macrophage foam cell formation via the scavenger receptor CD36 and is enriched in atherosclerotic lesions. J Biol Chem. 2002; 277:38517–38523. [PubMed: 12145296]
28. Piotrowski JJ, Shah S, Alexander JJ. Mature human atherosclerotic plaque contains peroxidized phosphatidylcholine as a major lipid peroxide. Life Sci. 1996; 58:735–740. [PubMed: 8632720]
29. Tsimikas S, Bergmark C, Beyer RW, et al. Temporal increases in plasma markers of oxidized low-density lipoprotein strongly reflect the presence of acute coronary syndromes. J Am Coll Cardiol. 2003; 41:360–70. [PubMed: 12575961]
30. Tsimikas S, Brilakis ES, Miller ER, et al. Oxidized phospholipids, Lp(a) lipoprotein, and coronary artery disease. N Engl J Med. 2005; 353:46–57. [PubMed: 16000355]
31. Tsimikas S, Willeit P, Willeit J, et al. Oxidation-specific biomarkers, prospective 15-year cardiovascular and stroke outcomes, and net reclassification of cardiovascular events. J Am Coll Cardiol. 2012; 60:2218–29. [PubMed: 23122790]
32. Cyrus T, Pratico D, Zhao L, et al. Absence of 12/15-lipoxygenase expression decreases lipid peroxidation and atherogenesis in apolipoprotein e-deficient mice. Circulation. 2001; 103:2277–82. [PubMed: 11342477]
33. Hutchins PM, Murphy RC. Cholesteryl ester acyl oxidation and remodeling in murine macrophages: formation of oxidized phosphatidylcholine. J Lipid Res. 2012; 53:1588–97. [PubMed: 22665166]
34. Romanoski CE, Che N, Yin F, et al. Network for activation of human endothelial cells by oxidized phospholipids. Circ Res. 2011; 109:E27–U52. [PubMed: 21737788]
35. Goldstein JA, Maini B, Dixon SR, et al. Detection of lipid-core plaques by intracoronary near-infrared spectroscopy identifies high risk of periprocedural myocardial infarction. Circ Cardiovasc interv. 2011; 4:429–37. [PubMed: 21972399]
36. Kini AS, Baber U, Kovacic JC, et al. Changes in plaque lipid content after short-term intensive versus standard statin therapy: the YELLOW trial (reduction in yellow plaque by aggressive lipid-lowering therapy). J Am Coll Cardiol. 2013; 62:21–9. [PubMed: 23644090]
37. Claessen BE, Maehara A, Fahy M, Xu K, Stone GW, Mintz GS. Plaque composition by intravascular ultrasound and distal embolization after percutaneous coronary intervention. J Am Coll Cardiol Img. 2012; 5:S111–8.
38. Stone GW, Maehara A, Lansky AJ, et al. A prospective natural-history study of coronary atherosclerosis. N Engl J Med. 2011; 364:226–35. [PubMed: 21247313]
39. Briley-Saebo KC, Nguyen TH, Saeboe AM, et al. In vivo detection of oxidation-specific epitopes in atherosclerotic lesions using biocompatible manganese molecular magnetic imaging probes. J Am Coll Cardiol. 2012; 59:616–26. [PubMed: 22300697]
40. Fang L, Green SR, Baek JS, et al. In vivo visualization and attenuation of oxidized lipid accumulation in hypercholesterolemic zebrafish. J Clin Invest. 2011; 121:4861–9. [PubMed: 22105168]
41. Torzewski M, Shaw PX, Han KR, et al. Reduced in vivo aortic uptake of radiolabeled oxidation-specific antibodies reflects changes in plaque composition consistent with plaque stabilization. Arterioscler Thromb Vasc Biol. 2004; 24:2307–12. [PubMed: 15528482]
42. Tsimikas S, Aikawa M, Miller FJ Jr. et al. Increased plasma oxidized phospholipid:apolipoprotein B-100 ratio with concomitant depletion of oxidized phospholipids from atherosclerotic lesions after dietary lipid-lowering: a potential biomarker of early atherosclerosis regression. Arterioscler Thromb Vasc Biol. 2007; 27:175–81. [PubMed: 17082490]
43. Tsimikas S, Miyanohara A, Hartvigsen K, et al. Human oxidation-specific antibodies reduce foam cell formation and atherosclerosis progression. J Am Coll Cardiol. 2011; 58:1715–27. [PubMed: 21982317]
44. Liu W, Yin H, Akazawa YO, Yoshida Y, Niki E, Porter NA. Ex vivo oxidation in tissue and plasma assays of hydroxyoctadecadienoates: Z,E/E,E stereoisomer ratios. Chem Res Toxicol. 2010; 23:986–95. [PubMed: 20423158]

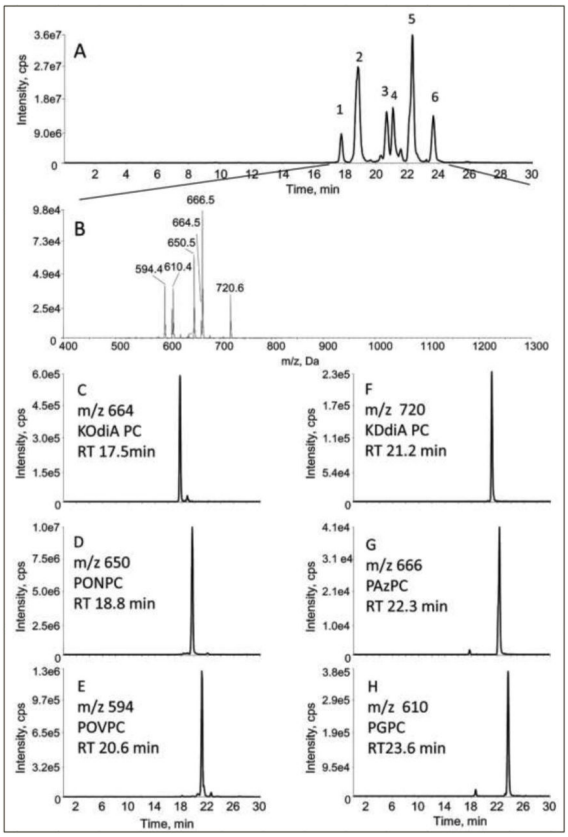

Figure 1.

Normal Phase LC-MS/MS analysis standard fragmented PX-OxPL molecules. (A) Total ion chromatogram from normal phase precursor ion scan (m/z 184) LC-MS/MS of 1 ng of each compound. KOdiAPC (peak 1), PONPC (Peak 2), POVPC (peak 3), KDiAPC (peak 4) PAzPC (peak 5), and PGPC (peak 6). (B) Averaged mass spectra of standard fragmented PC-OxPL molecules. Panels C-H represent ion chromatographs of the synthetic standards and their specific retention times. Calibration curves based on co injection with DNPC were done for each compound.

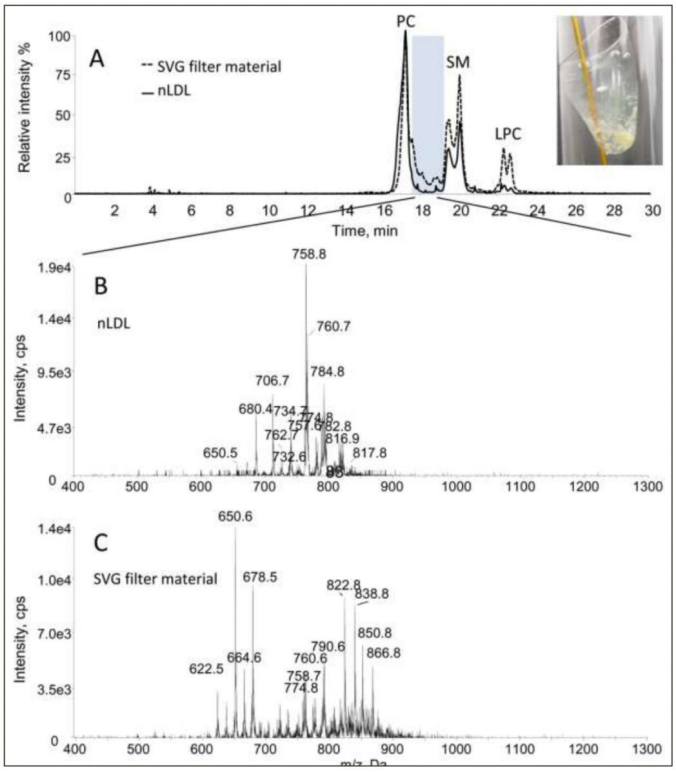

Figure 2.

Normal phase LC-MS/MS analysis of lipid extracts from SVG compared to native LDL. The filter with accompanying yellow debris is shown in the inset (A). Total ion chromatogram of precursor ions (m/z 184) for plaque material (dotted line) and native LDL (solid line). Mass spectra from retention time 17.5 till 19.2 min for native LDL (B) and (C) plaque material. PC= phosphatidylcholine, SM= sphingomeyelin, lysoPC= lysophosphatidylcholine.

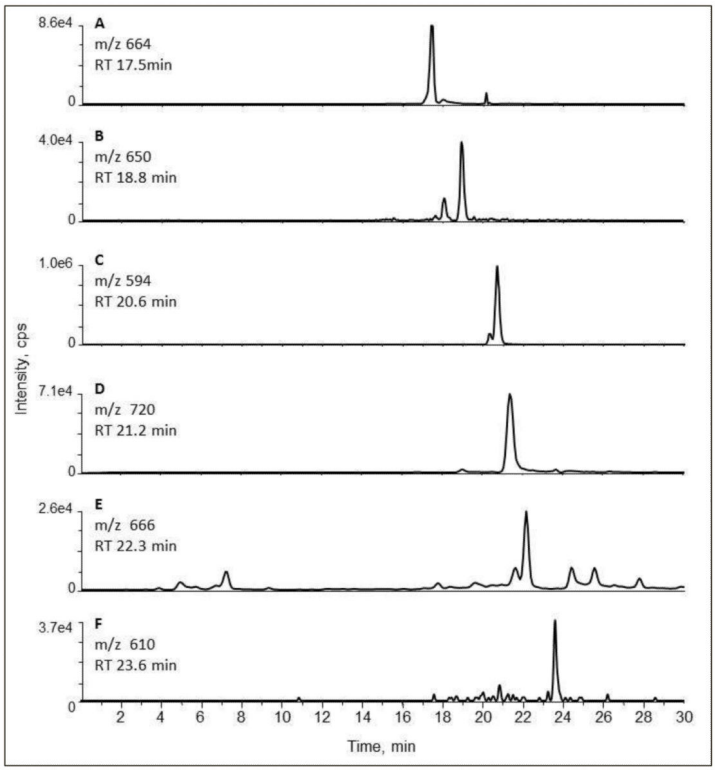

Figure 3.

Identification of PC-OxPL molecules within plaque material from filter retrieved from PCI in a Plaque material. Single ion chromatograms of fragmented PC-OxPL molecules within retrieved plaque material (A) KOdiAPC, (B) PONPC, (C) POVPC, (D) KDdiAPC, (E) PAzPC (F) PGPC. Retention times corresponded to known standards.

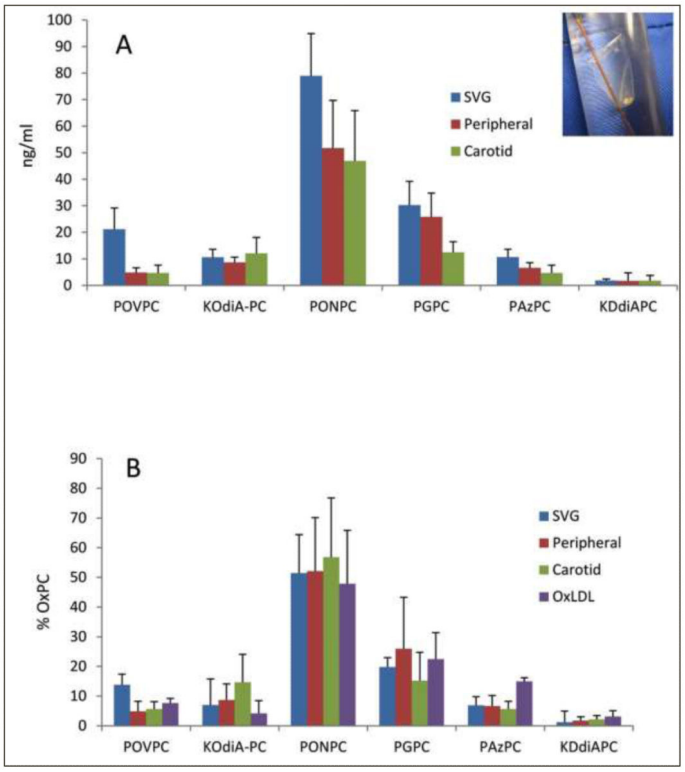

Figure 4.

Distribution of PC-OxPL recovered from distal protection filter devices from different vascular beds. (A) Concentration of PC-OxPL within different vascular beds based on dilution in 1 ml of PBS prior to extraction. Due to larger amounts of plaque recovery from SVG interventions there are higher levels of PC-OxPL within SVG samples. (B) Overall distribution of PC-OxPL from different vascular beds compared to OxLDL. All Samples were analyzed in triplicate in normal phase MRM LC/MS/MS (SVG n=5, Peripheral n=4, Carotid n=3)

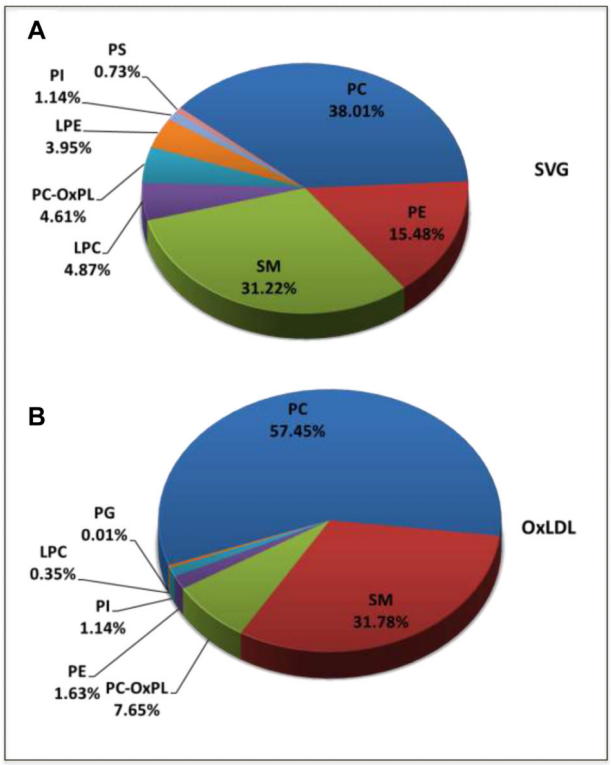

Figure 5.

Total phospholipid composition of filter material recovered from SVG interventions (A). The data represent an average of 4 samples analyzed in triplicate. Samples of OxLDL were also analyzed in triplicate by normal phase HPLC/MS/MS MRM scanning as a comparator (B). Phospholipid classes were quantitated based on class specific internal standards. % represents total Phospholipid. PC= phosphatidylcholine, SM= sphingomyelin, PE= phosphatidylethanolamine, LPC= lysophosphatidylcholine, LPE= lysophosphatidylethanolamine, PS= phosphatidylserine, PI= phosphatidylinositol, PG= phosphatidylglycerol.

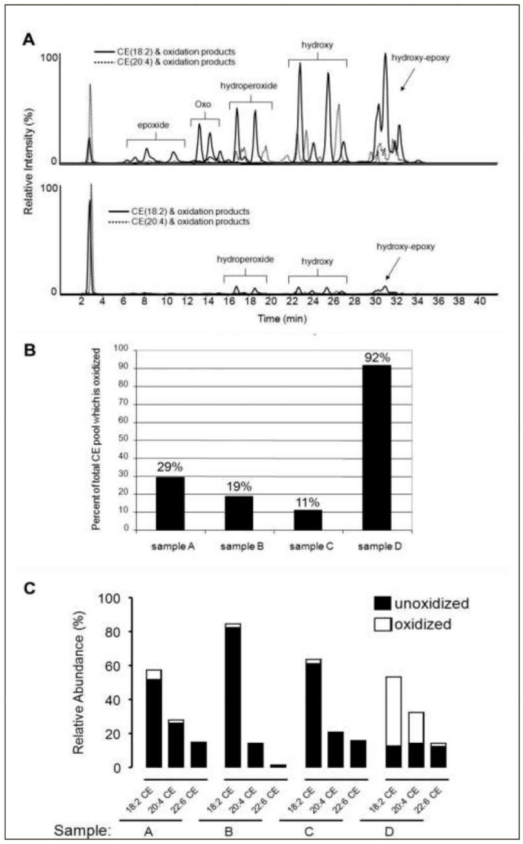

Figure 6.

Normal phase HPLC-MS/MS analysis of cholesteryl esters extracted from a distal protection filter following human saphenous vein graft procedure. Data were collected in multiple reaction monitoring mode (MRM). A- Solid chromatograms show CE(18:2) and it's oxidation products, dashed chromatograms represent CE(20:4) and it's oxidation products. Families of structurally related oxidation products are labeled with the characteristic oxygen moiety, e.g. the group of peaks labeled "hydroxy" are isomers of CE(HODE) (solid line) and CE(HETE) (dashed line). B- Estimated CE oxidation as a percent of the total CE pool in SVG filter device samples determined by peak area ratios of the three major CEs (18:2. 20:4, 22:6) and their various oxidation products by MRM analysis. C- Relative quantitation was assessed by NP-HPLC-MS/MS as described in Experimental Procedures. Solid bars indicate the relative abundance of the three major CE species; the summed oxidation products of each CE species are indicated by open bars.

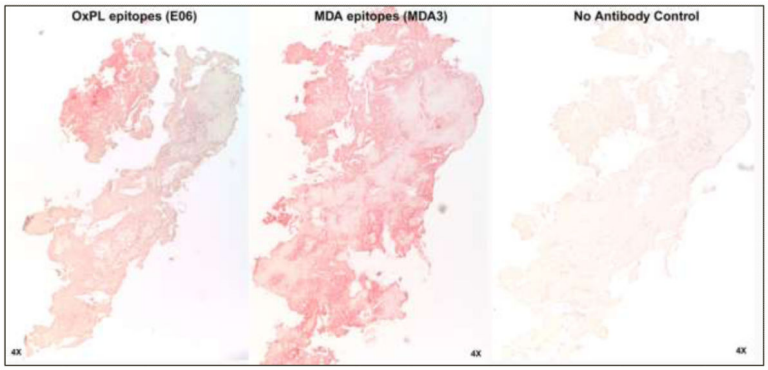

Figure 7.

Immunostaining of material derived from SVG filters for OxPL epitopes stained with antibody E06 and MDA epitopes stained with guinea pig polyclonal antibody MDA3.

Table 1

Embolic protection devices, vascular territory and baseline clinical characteristics of the patients undergoing percutaneous intervention from whom clinical were recorded.

Sample	Device	Vascular bed	Age	DM	HTN	↑Chol
1	Filter Wire	SVG	66	+	+	+
2	Filter Wire	SVG	65	−	+	+
3	Filter Wire	SVG	70	−	+	−
4	Filter Wire	SVG	69	+	+	+
5	Filter Wire	SVG	58	−	−	+
6	Filter Wire	Renal Artery	78	+	−	+
7	Filter Wire	Renal Artery	59	+	+	+
8	Spider	SFA	71	+	+	+
9	Spider	SFA	80	−	−	+
10	Accunet	Carotid	59	+	+	−
11	Accunet	Carotid	68	−	+	+
12	Accunet	Carotid	76	−	+	−